Mechanical properties of Al–8 wt % Fe-based alloys prepared by rapid quenching from the liquid state

G. THURSFIELD*, M. J. STOWELL
T.I. Research Laboratories, Hinxton Hall, Hinxton, Saffron Walden, Essex, UK

Aluminium-iron-based alloys have been prepared in bulk form from flakes that were splat-cast from the liquid. A detailed study has been made of the binary Al–8 wt % Fe alloy and the influence of several ternary additions is discussed. Mechanical properties of these materials are described and it is shown that the refinement in microstructure resulting from the extremely rapid cooling rates employed gives rise to improved mechanical behaviour, particularly in the temperature range 300 to 620K.

1. Introduction

The strength of aluminium alloys at elevated temperatures (<575K, 300°C, say), particularly of those with a high room temperature strength, is low when compared with that of other alloys (e.g. steels, Ti, Ni), and limits their application to temperatures below about 575K. The reduction in strength which occurs at higher temperatures is due to the thermal instability of the precipitates responsible for the strengthening effect.

Two general approaches for preparing dispersion-hardened aluminium alloys with improved elevated temperature stability have been established. The first approach depends on the external introduction of oxide, either by pre-oxidation of aluminium powder [1] or by blending aluminium and oxide powders [2]. The "sintered" aluminium powder products (SAP) retain strength up to the melting temperature, but have limited room temperature strength arising from an insufficiently small oxide barrier spacing, and reduced ductility at high temperatures, due to the opening of pores at oxide-aluminium interfaces [3]. Superimposed solid solution hardening increases the yield strength but at the expense of ductility [4]. The second approach involves the internal introduction of hard and stable intermetallic compounds by atomization of liquid aluminium alloys containing transition metal solutes, highly soluble in the liquid but highly insoluble in the solid. The use of these elements, notably Cr and Fe [5-7], has resulted in enhanced high temperature properties. Extrusions of atomized alloy powder based on Al–8% Fe† were shown by Towner [6, 7], to exhibit strength characteristics similar to SAP at temperatures of up to 675K, but with increased ductility at high temperatures. The strength of these dispersion-hardened alloys was limited by the intermetallic particle spacing of about 500 nm, deriving from the dendrite arm spacing within each atomized drop. Atomization techniques have also been used in recent years to give better wear and thermal expansion properties in piston materials by increasing the level of Si additions in Al–Si-based alloys [8]; and to give increased alloying in Al–Zn–Mg–Cu alloys to achieve higher yield strengths [9-11] (>700 MN m^{-2} in some cases) than can be achieved in conventionally prepared wrought materials.

Atomization depends on forced convection to achieve a cooling rate $\gtrsim 10^3$K sec^{-1}. The dendrite spacing can be further reduced, together with increased solid solubility and reduced segregation, by employing cooling rates ~10^5 to 10^6K sec^{-1} normally achieved by splat-cooling techniques. In splat-cooling processes the molten alloy is spread directly into foil or flake on a cold substrate through which heat is extracted by conduction, yielding enhanced solid

*Present address: Brookes (Oldbury) Ltd, Brades Road, Oldbury, Warley, Worcs., UK.
†All compositions are in wt %.

solubility, new metastable phases and, often, amorphous structures. Numerous property studies on aluminium and other alloys prepared by splat-cooling methods have been published during the last decade. These studies have been periodically reviewed, and three recent papers have adequately summarized the overall progress [12, 13], including specific investigations into the structure and properties of splat-cooled aluminium alloys [14].

Typically, the techniques used for preparing splat-cooled samples have been based on either the "gun" method [15] or the "piston-and-anvil" method [16], using equipment designed to melt and quench only a few drops of metal at a time. Consequently, the majority of the published work reports microstructural and microproperty studies on single flakes or foils with a geometry unsuitable for mechanical testing. Hence, there is a paucity of data on the mechanical properties of splat-cooled alloys. It has been possible, however, to extend the piston-and-anvil process to produce filamentary samples from which tensile data of the as-quenched material can be obtained [17, 18]. Esslinger [17], for example, produced such foils of Al–Mn, –Fe and –Si alloys, and showed that the tensile strength of the Al-Fe alloy was superior to that of Towner's atomized powder extrusions.

It is necessary to use splat-quenching techniques capable of producing commercially worthwhile quantities of material in order to exploit fully the advantages of very rapid cooling for alloy development. Such techniques are now available, and it is possible to fabricate bulk samples so that a detailed mechanical and physical property study can be carried out. Kaufmann and Muller, using a centrifugal atomization technique, showed that splat-cooling improved bulk mechanical properties by refining the grain size in beryllium alloys [19], and by dispersion-hardening in uranium [20] and zirconium [21] alloys. Centrifugal atomization has also been used to prepare splat-cooled Al–8 % Fe platelets, a few centimetres in diameter and up to 100 µm thick [22, 23]. Plasma-jet spraying has been used to produce dispersion-strengthened aluminium alloys, containing up to 4.9 % V [24, 25], in the form of 4 mm thick sheet. Methods which involve spraying molten alloy droplets formed by gas atomization against a rotating conductive substrate offer the most promise for the future developments. Lawrence and Foerster [26] demonstrated that splat-quenching of aluminium alloys containing liquid-soluble, solid-insoluble alloying additions could be achieved at rates $\sim$40 g sec^{-1}, by spraying an atomized stream against a revolving stainless steel disc. However, their technique suffered the disadvantage of not being able to remove the as-deposited flake continuously and consequently subsequent generations of droplets deposited on top of each other, leading to a reduction in the cooling rate as deposition progressed. Grant [27] employed a revolving water-cooled copper disc as the substrate, grit-blasted to improve thermal contact, to achieve some quite remarkable structural refinements and property improvements in alloy systems ranging from commercial aluminium alloys, through stainless steels to super alloys and high speed tool steels, and thus emphasized the important future role of splat-quenching techniques in alloy development.

Splat-quenched Al–Fe alloys have been the subject of much attention in recent years. It has been established [28] that the metastable solid solubility of Fe in Al is $\sim$10 % compared with an equilibrium solid solubility of 0.05 % Fe. Single splats of Al–Fe alloys containing 4 to 20 % Fe were shown by Jones [29] to contain two distinct structural zones, zone A and zone B, which were characterized by their response to etching in Keller's reagent. The lighter etching zone, designated zone A, was located at one or both surfaces, generally more frequently and extensively at the substrate side. The darker etching zone, designated zone B, occupied the remaining central regions. Either zone, however, could extend through the splat thickness, excluding the other. Jones showed the hardness of zone A to be at least twice that of zone B, with a discontinuity of hardness between the two zones. For Al- 8 % Fe the hardness of zone A was shown to be $\sim$260 kg mm^{-2} in comparison with $\sim$100 kg mm^{-2} for the zone B. A transmission electron microscopy study [30] of the splat-quenched Al–8 % Fe alloy showed zone A to consist of Al grains, saturated with Fe and containing a very fine network substructure of metastable iron-aluminium intermetallic particles, while in the zone B regions, particles of the equilibrium phase, $FeAl_3$, and the metastable phase, $FeAl_6$, were found embedded in the aluminium matrix. During annealing at temperatures >615 K, the fine-scale network of iron-aluminium intermetallic crystallites in the zone A regions decomposed to form semi-coherent needle-shaped $FeAl_3$ particles which subsequently coarsened at temperatures $\gtrsim 725$K to incoherent spheroidal shaped particles. The precipitation process has also been followed by measurements of the micro-hardness. The initially high hardness of zone A changed very little at annealing temperatures $\leqslant 575$K [29], while the onset of precipitation subsequently caused a large decrease in hardness [29, 31].

The present paper discusses the bulk production of rapidly cooled Al–Fe-based alloys, and the methods employed to fabricate bar stock from the splat-quenched flake. An earlier publication [32] described the high temperature tensile properties of the binary Al–Fe alloy and compared them with those of established high temperature aluminium alloys. These results are examined in more detail and, in addition, a range of mechanical and physical properties for this alloy are presented and discussed. The effects of adding a third alloying component on the properties of the Al–8% Fe alloy are also examined.

2. Experimental procedures

2.1. Material preparation

2.1.1. Production of alloys

The Al–8% Fe alloy ingots were produced directly from the pure components by the British Aluminium Co Ltd, and contained typically 0.04% Mn, 0.01% Si and 0.005% Cu as impurities. The Al–8% Fe–1% Zr alloy was prepared by alloying Al–8% Fe, Al–6% Zr master alloy supplied by B.A. Co Ltd, and high purity Fe supplied by BISRA. The alloy was melted in an argon atmosphere, and chill cast into a cylindrical copper mould, about 25 mm diameter and 125 mm high. The remaining ternary Al–8% Fe-based alloys used for this study were prepared in a similar manner by alloying Al–8% Fe, high purity Fe and the pure elemental components.

2.1.2. Splat-cooling and powder production

Individual splats for micro-hardness measurements were prepared by the "gun" technique. The equipment used was based on a published design [15], in which the melt was expelled from a graphite nozzle onto a grit-blasted copper substrate maintained at room temperature. The expelling shock wave was induced by subjecting a Mylar diaphragm, thickness 0.40 mm, to a steadily increasing argon pressure which burst it at $\sim$5 MN m^{-2}. Quenched foils had a mean thickness $\sim$0.030 mm with considerable thickness variations within single foils.

Bulk quantities of splat-quenched material were prepared by atomizing a stream of the molten alloy and then quenching the atomized droplets onto a rotating water-cooled copper drum, located at a predetermined distance vertically below the alloy reservoir crucible and the atomizing jets. Details of the design of the apparatus and the operational conditions required for the production of Al–8% Fe flake of consistent quality, containing a high proportion of zone A (normally $\gtrsim$60%), have been reported elsewhere [33]. This technique produced splats having an average diameter of approximately 10 mm and an average thickness of about 0.030 mm.

The material was prepared in $\sim$1.5kg batches. To ensure a high quality product, samples of each batch were examined by optical metallography and the average micro-hardness of the zone A areas was determined. Batches containing $<$60% zone A with a mean micro-hardness in the zone A areas $<$250kg mm^{-2} were rejected. (It has only been necessary to reject 5% of the $\sim$300 batches of Al–8% Fe produced so far.) The ternary Al–8% Fe based alloys, for which mechanical properties have been determined, were prepared in a similar manner.

The as-quenched flake was ground to yield a –150 mesh fraction by a rotary grinder consisting of a series of stellite-tipped high speed steel blades at right angles to each other. The grinding action was such that the splats were cut rather than milled, therefore minimizing the possibility of oxide formation. Ball milling was used to grind large batches of material, but it was found necessary to maintain an argon atmosphere in the milling chamber to prevent excessive oxide formation.

2.1.3. Compaction and extrusion

During the first phase of the programme, compaction and extrusion of the powder was carried out using a 0.5 MN Denison Universal press. The compaction/extrusion treatment comprised three stages, namely: (i) compaction of the powder in 15 mm diameter, 32 mm high aluminium cans at ambient temperatures, to obtain a "green" billet with a density of $\sim$80% of the theoretical density: (ii) re-compaction of the green billet, after removing the can by machining, to obtain a high density billet (a minimum density ~95% of the theoretical density was achieved in practice): (iii) extrusion of the billet at a series of temperatures between 525 K and 650 K and through a series of different sized dies, in order to determine the effects of extrusion temperature and extrusion ratio on the mechanical properties. A series of experiments was carried out to determine the optimum compaction and extrusion temperatures required to produce extrusions having high room temperature and elevated temperature tensile strengths together with a commercially viable ductility (assumed to be ~5%). The optimized compaction and extrusion temperatures were then used in the second phase of the programme in which larger diameter extrusions were prepared and tested.

A 3 MN laboratory press, capable of compacting and extruding billets up to 50 mm diameter, was used to obtain extruded bar up to 19 mm diameter. The route for preparing these extrusions was similar to that described above.

In each of the compaction and extrusion treatments described, a suspension of graphite in white spirit was applied to those surfaces of the press tooling which came in contact with the billets and to the outer surfaces of the billets, or to the outer surfaces of the cans used in the cold compaction processes.

2.2. Determination of mechanical properties

2.2.1. *Hardness measurements*

Micro-hardness measurements were made made with a 0.1 N (10 g) load using Reichert and Leitz equipment. Measurements were made on splats in the as-quenched condition, and after annealing for 1 h at 375 K in a bath containing ethylene glycol solution, and at a range of temperatures between 425 K and 725 K in Cassel TS-150 aluminium salt solution.

Since the structures studied contained normal casting defects, particularly porosity, measurements were restricted to areas for which no such defects were indicated by etching. Untypically low micro-hardness values were also rejected on the assumption that sub-surface defects were responsible. Each value quoted is the mean of 12 remaining measurements. Increasing the number of measurements to 100 in test cases did not significantly reduce the standard deviation from the mean, which indicates that the range of hardness values obtained reflected variations in as-cast microstructure rather than errors in measurement.

Macro-hardness measurements were carried out on transverse sections of extruded bar, both in the as-extruded condition and after annealing, under the conditions described for single splats. The measurements reported were made at 2.15 kN load using a Vickers' Pyramid hardness tester.

2.2.2. *Tensile testing*

Testing of extruded bar up to 3.2 mm diameter, prepared on the Denison press, was carried out on an Instron testing machine (model TT-C-L) at a constant cross-head velocity of 0.004 mm sec^{-1}.

Elevated-temperature tensile tests were carried out after soaking the specimens for 1, 100 and 1000 h at the testing temperature. Specimens tested after 1 h at the test temperature were heated in a triple-wound furnace in which a constant temperature zone (±2K) ~130 mm long was maintained. Specimens tested after 100 and 1000 h at the test temperature were first soaked for 99 and 999 h respectively at the test temperature in either ethylene glycol solution (for specimens tested at 375 K) or Cassel TS-150 aluminium salt solution (for specimens tested at temperatures ⩾425 K). The specimens were then tested after being soaked for a further 1 h in the furnace described above. The room temperature tensile properties were also determined for Al–8% Fe specimens, annealed for 1 h at temperatures between 375 and 655 K. With Al–8% Fe specimens, several tests were carried out for each heat-treatment condition. Normally only one sample of alloys with ternary additions was tested.

Tensile tests were carried out on 3.2 mm diameter specimens having a 16.5 mm gauge length machined from small extrusions of ~5.5 mm diameter and on specimens machined to BS 18:1970 specification from larger bars of 19 mm diameter. Comparisons were made between the Al–8% Fe alloys and RR57 (Al–6% Cu based), RR58 (Al–2% Cu–1.5% Mg–Fe–Ni) and RR77 (Al–5.5%Zn–3%Mg–Cu) which were supplied in the fully hardened condition by High Duty Alloys Ltd.

3. Results

3.1. Hardness data

3.1.1. *Al–8% Fe*

The micro-hardnesses of the zone A and zone B regions in Al–8% Fe splats prepared by the gun technique are plotted in Fig. 1 as functions of the annealing temperature. These results were obtained by Jones [29], and have been confirmed in the present work. Specimens were annealed for 1 h prior to testing at room temperature.

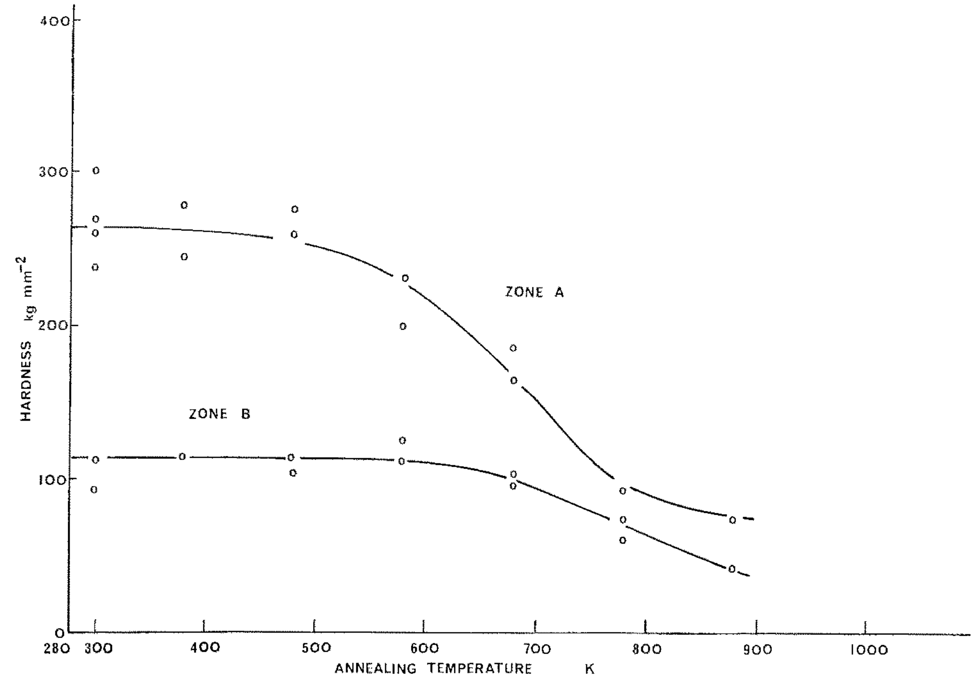

Figure 1 Micro-hardness of the zone A and zone B regions in Al–8% Fe "gun" splats as a function of annealing temperature. Each specimen was annealed for 1 h prior to each test (after Jones [29]).

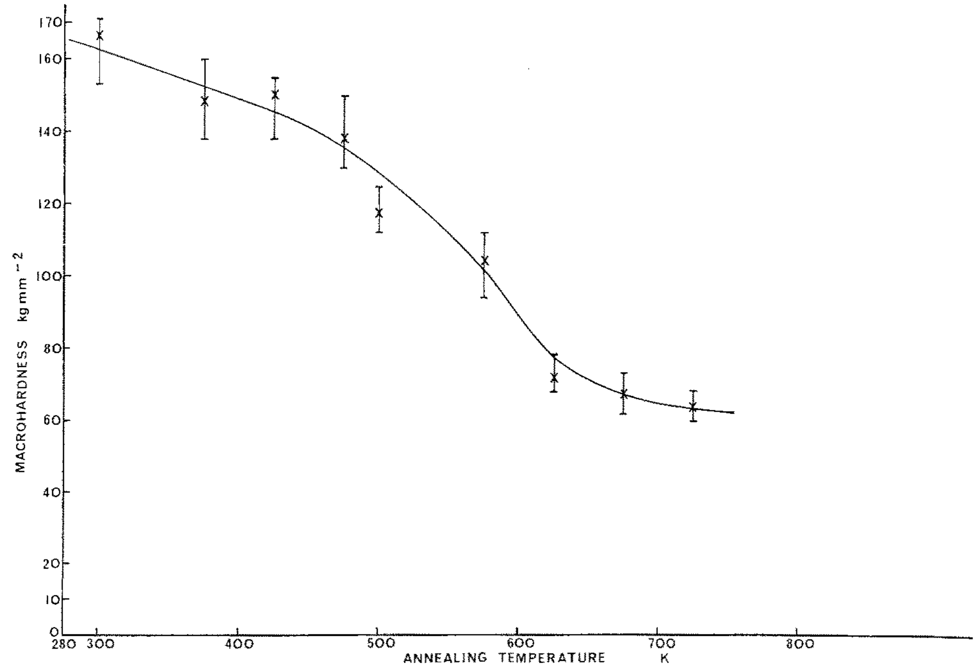

Figure 2 Macro-hardness data for Al–8% Fe extrusions. Measurements were made on transverse sections annealed for 1 h prior to each test. The data plotted represents the mean of 12 measured values.

The hardness of the zone A regions was found to be about 2.5 times the zone B hardness in as-quenched splats, the hardness of zone B approaching values obtained for Al–8 % Fe chill castings. The zone A hardness showed no further change after annealing for at least 100 h at temperatures up to ~575K. The decrease in hardness of zone A between 575 and 675K is associated with the decomposition of the fine scale network of iron-aluminium intermetallic crystallites to coherent needle-shaped $FeAl_3$ particles. The $FeAl_3$ needles coarsen rapidly at $\gtrsim$725K [30, 35] and this results in a further reduction in microhardness.

The macro-hardness of transverse sections of 19 mm diameter Al–8 % Fe extrusions, prepared by extruding at 575K, is plotted as a function of annealing temperature in Fig. 2. The results predict a yield stress ~508 MN m^{-2} at room temperature and ~315 MN m^{-2} at 575K, assuming the approximate relation $H_V \simeq 3\sigma_Y$ [36], where H_V is the Vickers hardness and σ_Y is the yield strength of the material. This result should be compared with data for the 0.1 % proof strength of the alloy given in Section 3.2.

3.1.2. Al–8 % Fe + ternary additions

It was hoped that certain ternary additions to Al–8 % Fe might postpone the decomposition of the network phase in zone A to higher temperatures than observed in the binary alloy, so as to provide a high strength at temperatures $\gtrsim$ 725K. A preliminary study was made of the effects of several additions on the micro-hardness of zone A regions in (a) as-quenched splats and (b) splats annealed for 1 h at a series of temperatures between 375K and 725K. Six different alloys were explored, having: (1) to (4), 1 % additions of Zr, Mn, Cr and Ni, (5) a 1 % total addition of Cr, V, W and Zr (thus giving an alloy composition equivalent to the strongest Al–7.6 % Fe-based alloy (M486) described by Towner [6]) and (6) a 1 % total addition of Cr, V, Ti and Zr. The results of this investigation are given in Fig. 3.

It will be seen that a 1 % Zr addition increases the micro-hardness at all temperatures in the range considered, and particularly between 600 and 725K. The Al–8 % Fe–1 % Mn alloy had a significantly higher hardness than Al–8 % Fe between 425K and 625K, but a reduced hardness at higher temperatures. Each of the other alloys considered gave a reduced hardness at temperatures $\gtrsim$ 550K. Increasing the addition of Mn to 3 % brought about a marked increase in hardness particularly between 425 and 625K (Fig. 4). Filamentary samples of Al–8 % Fe–3 % Mn were previously shown by Esslinger [17] to have a thermal stability in the temperature range 425 to 625K superior to all conventional Al materials, including SAP. Reducing the Mn addition to 0.5 % did not result in a significant change in the zone A micro-hardness (Fig. 4) over that obtained in Al–8 % Fe.

It is significant to note that the average micro-hardness value for the zone B areas of Al–8 % Fe–3 % Mn splats in the as-quenched condition was 142 kg mm^{-2}. This result is to be compared with ~ 100 kg mm^{-2} for Al–8 % Fe (Fig. 1). Mn additions up to ~ 1 % do not bring about any significant change in zone B hardness. The zone B areas in the Al–8 % Fe–3 % Mn alloy contain a significant volume of a eutectic-like phase, in the form of rod-shaped particles [37]. The occurrence of this phase could account for the higher hardness obtained in zone B for this alloy, and possibly the unexpectedly low micro-hardness values obtained for the zone A areas in as-quenched splats.

3.2. Room temperature and elevated temperature tensile properties

3.2.1. Optimization of extrusion conditions

Detailed transmission electron microscope studies [30, 35] and micro-hardness data (Section 3.1) show that the network structure in the zone A regions of Al–8 % Fe splats begins to coarsen at temperatures $\gtrsim$ 615K. Since the as-quenched microstructure cannot be recovered by heat-treatment, it follows that it is essential to maintain operating temperatures during compaction and extrusion (or, indeed, when subjecting the alloy to any metal-forming operation) to < 615K to preserve the beneficial microstructures and properties obtained by splat-cooling.

To illustrate this point, tensile tests were carried out on specimens machined from 5.5 mm diameter extrusions, prepared from 15 mm diameter billets (E.R. 8:1), using a range of extrusion temperatures from 525 to 725K. The results of this study are given in Fig. 5, in which the ultimate tensile strength and the percentage elongation to fracture are plotted as functions of extrusion temperature. A progressive reduction in tensile strength, together with increased ductility, is observed with increasing extrusion temperature. Extrusion at 525K

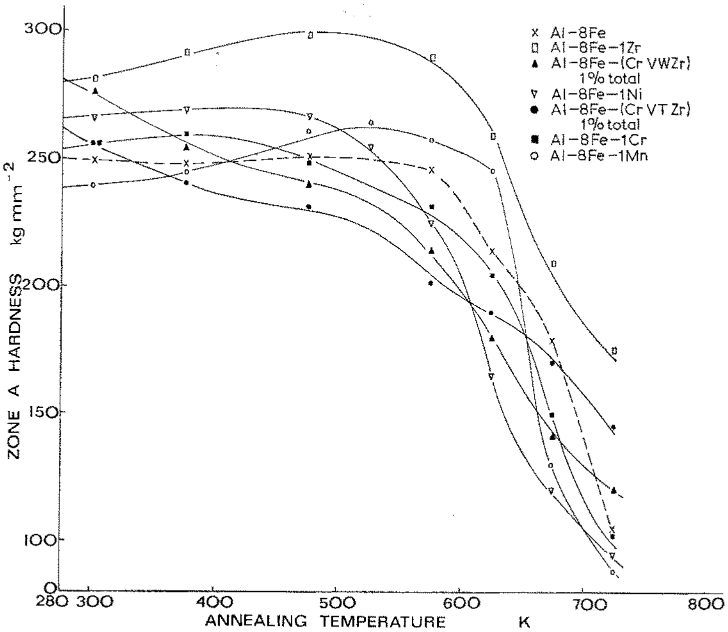

Figure 3 A comparison of the micro-hardness of the zone A areas in ternary alloys based on Al–8% Fe with the binary Al–8% Fe alloy. Each sample was annealed for 1 h prior to each test. The maximum deviation from the plotted values was ± 42 kg mm^{-2}.

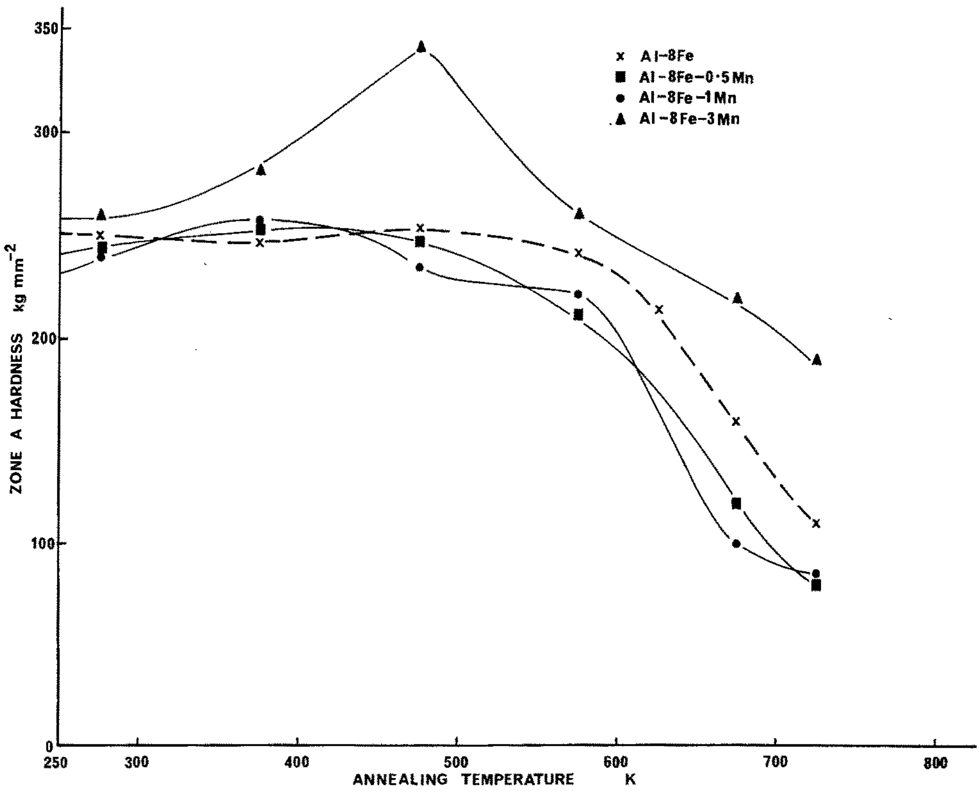

Figure 4 A comparison of the micro-hardness of the zone A areas in ternary Al–Fe–Mn alloys with the binary Al–8% Fe alloy. Each sample was annealed for 1 h prior to each test. The maximum deviation from the plotted values was ± 35 kg mm^{-2}.

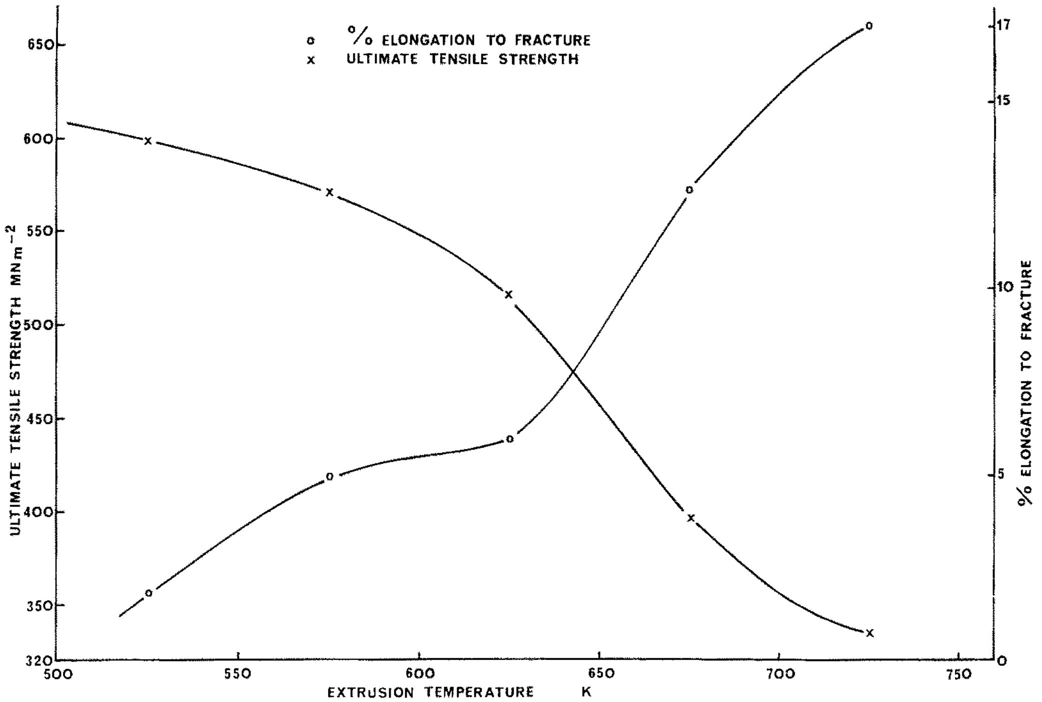

Figure 5 The ultimate tensile strength and ductility of 5.55 mm diameter Al–8% Fe extrusions as functions of extrusion temperature. The extrusions were prepared from 15 mm diameter billets (extrusion ratio 8:1).

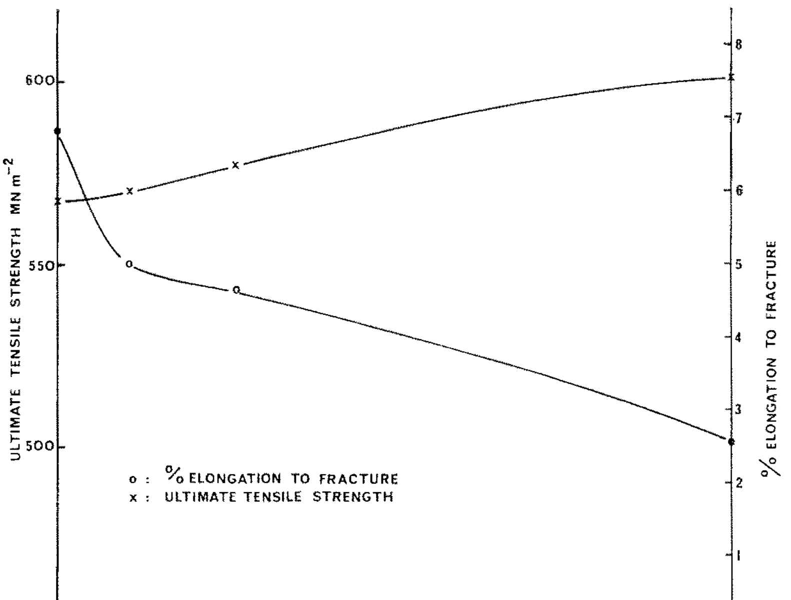

Figure 6 The ultimate tensile strength and ductility of Al–8% Fe extrusions prepared from 15 mm billets at 575K as functions of extrusion ratio.

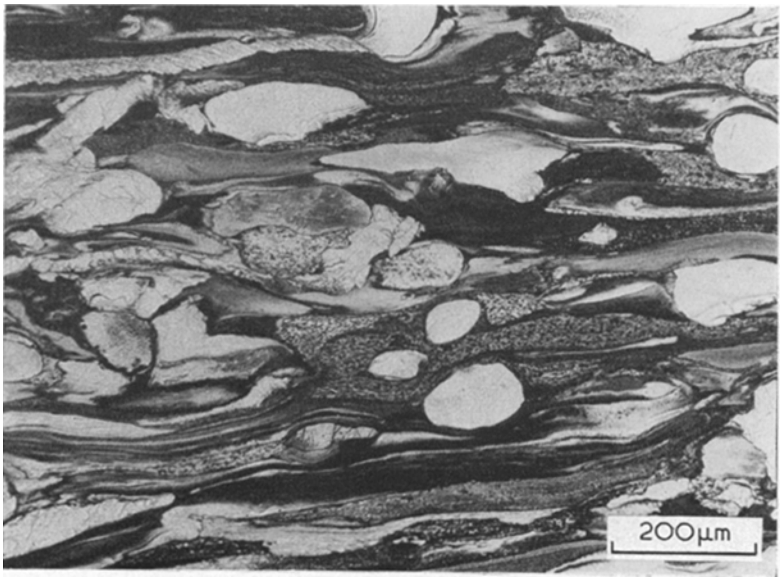

Figure 7 Longitudinal section through Al–8% Fe extrusion. Material extruded at 575K with an extrusion ratio 8:1.

gave the highest tensile strength (598 MN m^{-2}), but a ductility (1.8%) less than that which can be considered to be commercially viable. Extrusion at 575K gave the optimum combination of strength (570 MN m^{-2}) with ductility (5% elongation to fracture). Specimens machined from extrusion prepared at 725K had an ultimate tensile strength of 335 MN m^{-2}, with 17% elongation to fracture, which is similar to that obtained by Towner [6, 7] for atomized Al–7.6% Fe, and by Ahlborn and Merz [22], who extruded centrifugally atomized Al–8% Fe at 655K.

The ultimate tensile strength of Al–8% Fe was dependent on the extrusion ratio (Fig. 6). A progressive increase in the ultimate tensile strength and a progressive reduction in the ductility are observed with increasing extrusion ratio. However, an extrusion ratio of 25:1 was difficult to achieve at 575K and an extrusion ratio of 6:1 produced, in some cases, unsound bar. Extrusion of Al–8% Fe generally occurs by deformation of the softer zone B regions around the hard zone A regions (Fig. 7). To obtain a sound extrusion, particularly free from internal defects, some deformation of zone A must take place. In the absence of some deformation of the zone A regions, the particle-particle bonding is reduced in extrusions, resulting in internal defects. The forces required to achieve a reduction ratio of 6:1 did not permit the necessary deformation of zone A and hence, an unsound product was obtained.

3.2.2. *Al–8% Fe tensile properties*

Fig. 8 describes the ultimate tensile strength, 0.1% proof stress, modulus of elasticity and percentage elongation to fracture of Al–8% Fe specimens, machined from a 5.5 mm extrusion, after 100 h exposure at the test temperature, measured at room temperature. At ambient temperatures the alloy possesses a minimum ultimate tensile strength of 570 MN m^{-2} and a minimum 0.1% proof strength of 503 MN m^{-2}, with 5% elongation to fracture. The minimum ultimate tensile strength at 575K is 232 MN m^{-2}, with a minimum 0.1% proof stress of 214 MN m^{-2} and 11.5% ductility. The observed reduction in strength between room temperature and $\sim$ 575K is closely related to the reduction in modulus with increasing temperature.

The properties after 100 h and 1000 h at the testing temperature do not vary significantly from those soaked for 1 h. The 1 h tensile strengths were only $\sim$ 5% greater than the 100 h tensile strengths.

The results for Al–8% Fe were compared with those determined under equivalent conditions for three established high temperature aluminium alloys: RR57, RR58 and RR77. Fig. 9 compares the 100 h ultimate tensile

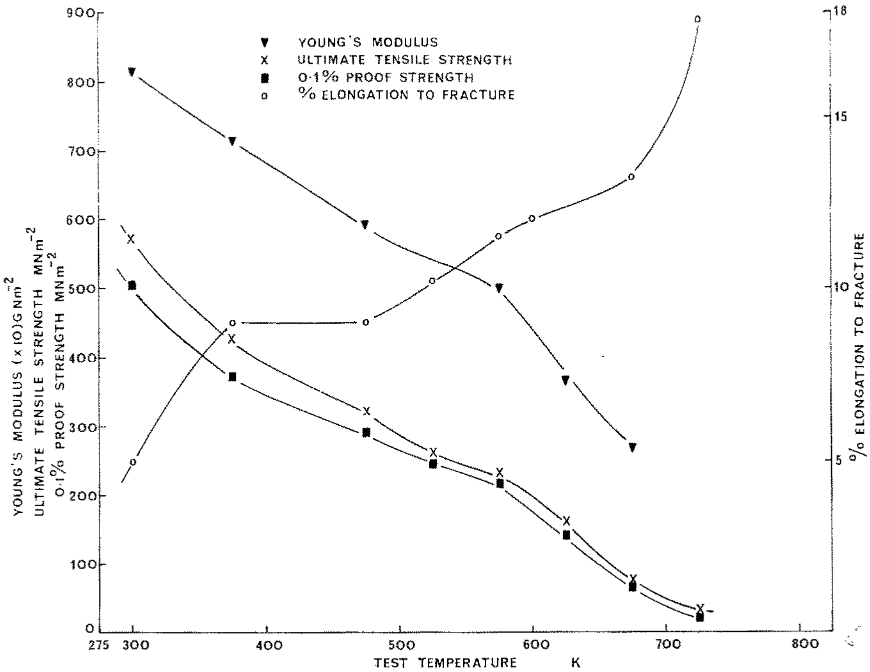

Figure 8 The ultimate tensile strength, 0.1% proof strength and ductility of Al–8% Fe as functions of the test temperature. Each specimen was soaked at the test temperature for 100 h.

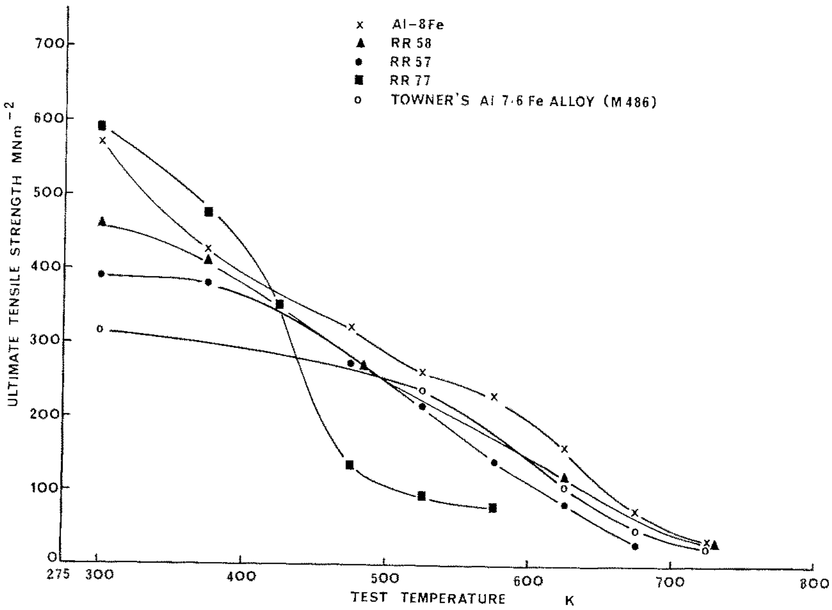

Figure 9 A comparison of the ultimate tensile strength of splat-quenched Al–8% Fe, RR58, RR57, RR77 and Towner's [6] atomized Al–7.6% Fe based alloy after 100 h at the test temperature.

strength of these alloys with Al–8% Fe at temperatures up to 725 K, and with the atomized Al–7.6% Fe alloy developed by Towner [6, 7]. It will be seen that the splat-quenched Al–8% Fe alloy has superior high-temperature properties both to RR77, which has equivalent room-temperature properties, and to RR57 and RR58, which possess inferior room-temperature proper-

TABLE I Comparison of published data for the ultimate tensile strength of Al–8% Fe at room temperature

Alloy	Reference	UTS (MN m^{-2})
Al–8% Fe (gas-atomized)	5	360
M486 (Al–7.6% Fe) (gas-atomized)	6, 7	315
Al–8% Fe: splat-quenched by centrifugal atomization	22	356
Al–8% Fe: ribbon foil produced by the "piston-and-anvil" technique	17	498
Al–8% Fe: splat-quenched by gas-atomization/spray-quenching	present work	570

ties. The strength of the splat-quenched Al–8% Fe alloy is significantly superior to that of Towner's atomized alloy at all temperatures up to ~675K. At 725K the two alloys have comparable properties. This result is consistent with microstructural observations [30, 35], since at 725K the splat-quenched Al–8% Fe alloy has a predominantly zone B type structure, similar to that reported by Towner for his as-atomized material.

Table I compares the ultimate tensile strength of the splat-quenched Al–8% Fe alloy with those of Al–8% Fe alloys prepared by gas atomization [5, 6], centrifugal atomization followed by splat-quenching [22], and a "clashing mould" technique [17] (similar to the piston-and-anvil process). The low tensile strength of the Al–8% Fe alloy described by Ahlborn and Merz [22] may be accounted for by noting that their alloy was extruded at 653K (i.e. at a temperature above which the network structure is known to coarsen) and that the cooling rate in their apparatus was probably substantially below ~ 10^6 K sec^{-1}, because a polished substrate was preferred to an abraded surface.

3.2.3. Al–8% Fe – effect of annealing on room temperature properties

Fig. 10 describes the room temperature ultimate tensile strength and ductility as functions of the annealing temperature. Tests were carried out on specimens prepared from bars extruded at 525K. A slight increase in the tensile strength with increasing annealing temperature is observed up to ~615K, followed by a significant reduction in strength. The results emphasize the stability of the zone A microstructure up to 615K. The increase in strength between 585K

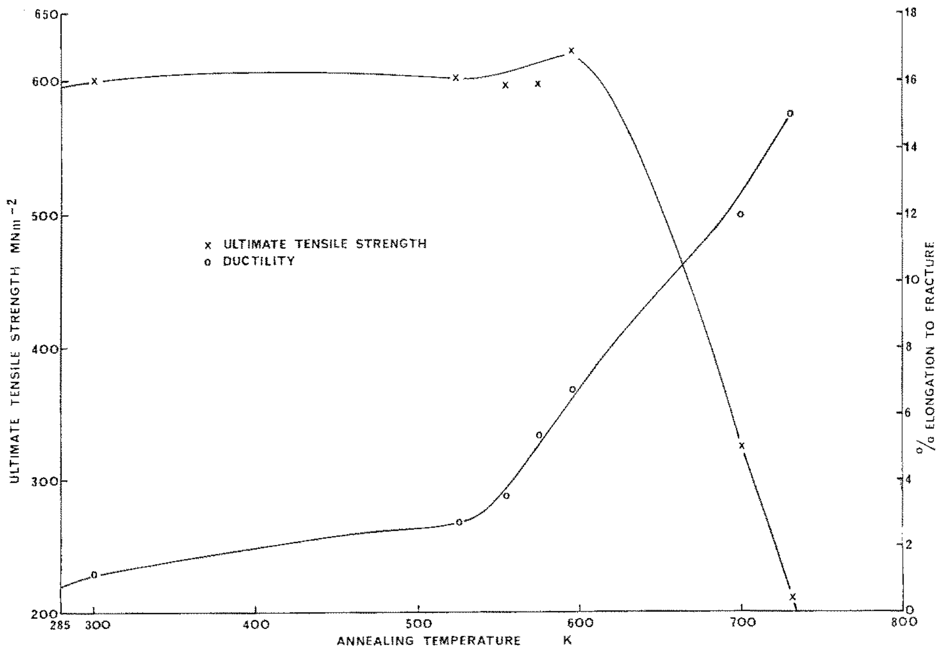

Figure 10 Room temperature ultimate tensile strength and ductility as functions of annealing temperature. Specimens were prepared from bar extruded at 525K.

and 615K can be attributed to some precipitation-hardening taking place during annealing within this temperature range. The reduction in strength following annealing at temperatures > 615K is closely related to the observed reduction in the zone A micro-hardness (Fig. 2).

3.2.4. *Al–8% Fe + ternary additions*

In Section 3.1 it was shown that, of the ternary elements considered, 1% additions of Zr or Mn to the binary Al–8% Fe alloy had the most significant effect on the micro-hardness of the zone A regions, and a 3% Mn addition to Al–8% Fe resulted in a 50% increase in the micro-hardness of the zone B areas of as-quenched splats. To determine the effects of the Mn and Zr additions on the tensile properties of Al–8% Fe, tensile specimens, machined from the 5.5 mm diameter extrusions of the Al–5% Fe–3% Mn, Al–8% Fe–1% Mn, Al–8% Fe–3% Mn and the Al–8% Fe–1% Zr alloys, were tested at room temperature, and after exposure at temperatures up to 725K for times up to 100 h.

The ultimate tensile strengths, elongations to failure and 0.1% proof stresses of these alloys after 100 h at temperature are shown in Figs. 11, 12 and 13 respectively. It is seen that the Al–8% Fe–1% Zr alloy has a superior U.T.S. and 0.1% proof stress to the binary alloy at all temperatures but is significantly less ductile up to about 650K. The Al–8% Fe–Mn alloys are slightly stronger than the binary alloy and less ductile below 550K but rapidly lose strength at higher temperatures. The Al–5% Fe–3% Mn alloy is generally inferior to Al–8% Fe over the whole temperature range.

It is evident from these results that improvements in UTS and 0.1% proof stress can be obtained by additions of Zr and Mn to Al–8% Fe although, unfortunately, these benefits are achieved at the expense of ductility. To achieve commercial viability, improved ductility could be brought about by changes in composition or processing conditions, albeit at the expense of some strength.

The Al–8% Fe–3% Mn alloy extrusions have an inferior strength to the Al–8% Fe–3% Mn foils prepared by Esslinger [17] (see Fig. 11), particularly at temperatures > 575K. This suggests that some loss in strength occurred as a consequence of compaction and extrusion; Esslinger tested as-splatted material which received no further processing.

3.3. Other mechanical properties

Creep tests were carried out on 5.06 mm

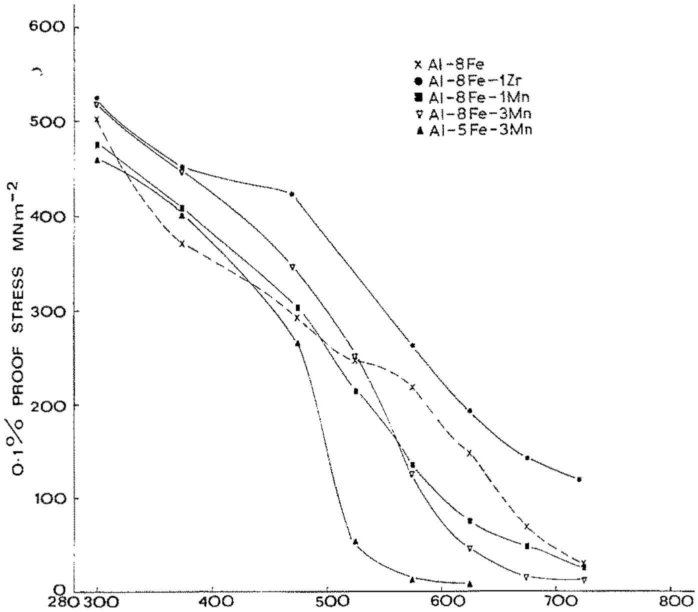

Figure 11 Comparison of the 100 h ultimate tensile strengths of the Al–Fe–Mn alloys with those for Al–8% Fe–1% Zr and Al–8% Fe. The results are compared with data for splat-quenched Al–8% Fe–3% Mn foils prepared by Esslinger [17].

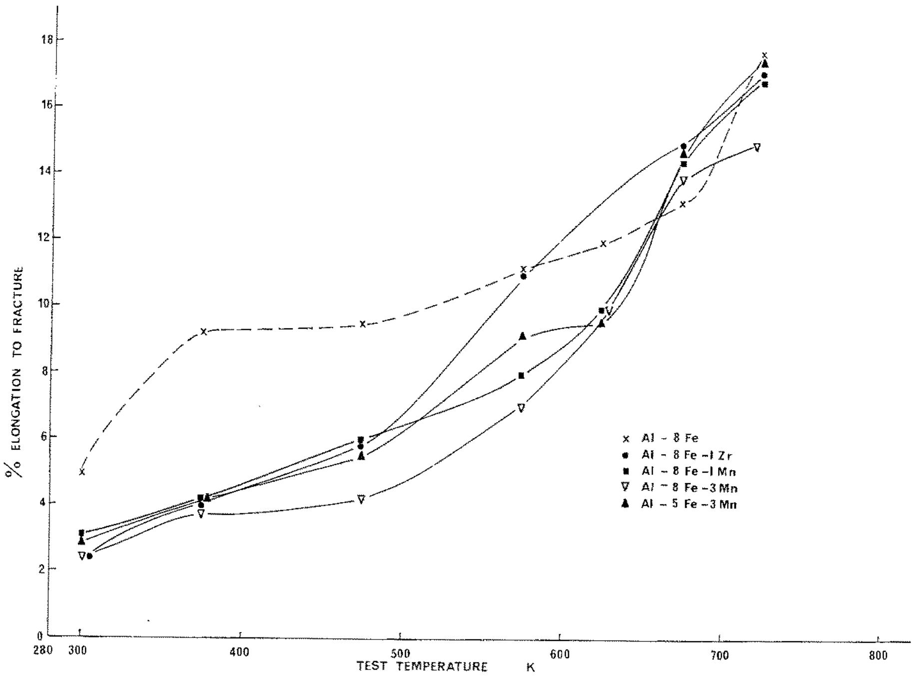

Figure 12 Comparison of the ductility data for the Al–Fe–Mn alloys with those for Al–8% Fe–1% Zr and Al–8% Fe. Each specimen was exposed for 100 h at the test temperature.

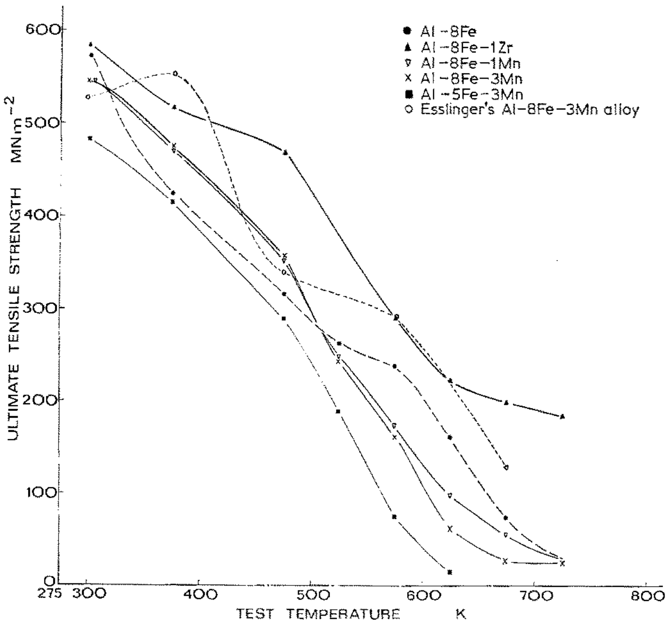

Figure 13 Comparison of the 0.1% proof stress of the Al–8% Fe–Mn alloys under test with values obtained for the Al–8% Fe–1% Zr and Al–8% Fe alloys. Each specimen was exposed for 100 h at the test temperature.

diameter specimens with a 35 mm gauge length on a BNFMRA apparatus with a lever loading frame. (These tests were executed by Mr G. Fowler of Magnesium Elektron Ltd.) Testing was carried out for periods up to 1000 h at 425, 475, 525, 575 and 625K. The stresses required

TABLE II Comparison of creep data for Al–8% Fe and RR58

Temperature (K)	Stress ($MN\ m^{-2}$)	RR58 Time to stated strain (h)			Al–8% Fe Time to stated strain (h)		
		0.1 %	0.2 %	0.5 %	0.1 %	0.2 %	0.5 %
425	284	No data	30	65	55	215	> 1000
	356		No data		< 1	65	ruptured at 0.46% strain
475	193	35	85	190	17.5	140	880
	254		No data		0.125% initial strain	20	ruptured at 0.35% strain
525	99	55	115	240	87	390	> 1000
	108	35	120	140	30	170	700
575	86		No data		40	250	~ 1000
	124		No data		0.145% initial strain	35	ruptured at 0.47% strain

TABLE III Impact values for Al–8% Fe, RR77 and RR58

	Energy to failure (J) Notched	Energy to failure (J) Un-notched
Al–8% Fe	19.40	34.00
RR77	20.20	34.70
RR58	23.20	37.70

TABLE IV Stress corrosion life. Life at 95% of 0.1% proof stress

	Time to failure (h)	Applied stress ($MN\ m^{-2}$)
Al–8% Fe	2183 ± 178	480
RR77	1437 ± 40	495

to produce 0.1, 0.2 and 0.5% total plastic strain in 1 h, 100 and 1000 h were deduced and the results are compared with published data [34] for RR58 in Table II. Al–8% Fe is seen to be significantly more resistant to creep failure at all temperatures up to 575 K.

The energy to failure of notched and un-notched samples, 8 mm in diameter, was obtained on Hounsfield impact testing equipment. Notches were 45°, 21 mm deep with a root radius < 2 mm. Table III gives the results of these tests for Al–8% Fe and for RR77 and RR58 Hounsfield specimens tested in the same equipment. Al–8% Fe is seen to have comparable impact properties to both of the commercial alloys.

Accelerated stress-corrosion tests were conducted on Al–8% Fe tensile specimens, machined to BS18:1962 specification, at room temperature. A stress equivalent to 95% of the 0.1% proof stress was applied to specimens that were fully enclosed in plastic containers and sprayed with a 1% NaCl solution every 12 h. Times to failure on these, and on equivalent RR77 specimens, were measured and are compared in Table IV. It is seen that Al–8% Fe is superior to RR77. The general corrosion behaviour of Al–8% Fe was not examined.

4. Discussion

The alloys described in this paper have been shown to have outstanding high temperature and room temperature properties. The high temperature properties are derived from the extremely stable microstructures which prevail at temperatures up to about 615 K. The outstanding strength and high-temperature stability of these alloys is derived from the high supersaturations and the extremely fine microstructures in the zone A regions, the occurrence of which can be directly attributed to the cooling rates obtained in splat-cooling. The results for Al–8% Fe based alloys thus exemplify the sort of results that can be achieved by splat-cooling, hence demonstrating the important future role of this technique in alloy development. In recent years, this development has been restricted to the examination of microstructures and the determination of micro-property data of alloys prepared by "single-splat" techniques. Now, with the advent of bulk splat-cooling processes, similar to the gas-atomization/spray-quenching technique used in this work, the preparation of a host of hitherto unconsidered alloys for commercial use is a sound practical proposition. Further, there is no reason why splat-cooling techniques cannot be used to improve the properties of many existing commercial alloys. This possibility has already been examined by Grant [27], who achieved significant improvements in the fatigue properties of the 2024 aluminium alloy (Al–4.5% Cu–1.5% Mg–Mn, Fe, Si) using a rotating wheel technique.

Micro-hardness data determined at room temperature for the zone A and zone B areas in single Al–8% Fe splats, annealed for 1 h at temperatures up to 725K, suggest that the room temperature strength should be retained for annealing temperatures up to 575K, with a gradual reduction in strength above this temperature (Fig. 1). Results for the room temperature strength as a function of annealing temperature (Fig. 10) confirm this trend. However, the tensile strength and 0.1% proof strength are shown to decrease with increasing temperature (Fig. 8), the proof strength being closely allied to the macro-hardness values given in Fig. 2. The reduction in the proof strength and the ultimate tensile strength is also closely related to the reduction in Young's modulus.

The reduction in zone A hardness above 575K has been attributed to the decomposition to $FeAl_3$ needles of the iron-aluminium crystallites which form the fine network structures which subsequently coarsen above about 655K to spherical particles. The coarsening of the network structure can also explain the reduction in room temperature strength in Al–8% Fe observed when the alloy is extruded at temperatures above $\sim$575K (Fig. 5). The reduction in strength and *macro*hardness, and increased ductility, between room temperature and 575K, are less easy to explain in terms of the observed microstructures. The microstructural behaviour of extrusions after annealing is essentially the same as that observed in single splats [35]; the network structure in zone A remains stable up to 575K, with decomposition of the iron-aluminium crystallites above this temperature to form $FeAl_3$. The results in Fig. 8 thus indicate that the reduction in strength and increase in ductility between room temperature and 575K is more likely a consequence of the observed reduction in Young's modulus. The effect of temperature on the bonding between particles in extrusions may also contribute to the observed decrease in strength, as may the presence of oxide layers between the particles. (Chemical analysis shows that oxygen pickup during the preparation of extrusions is low: <100 ppm). These factors have not been examined in any detail, although it is known that specimens invariably fail at particle boundaries, and that excessive amounts of oxide can lead to reduced ductility and premature failure.

The higher room temperature strength of the Al–8% Fe–1% Zr alloy, compared to the binary alloy, is considered to result from three factors [35]: (i) the second-phase network spacing was finer, (ii) the whole of the 1% Zr addition was held in solid solution and (iii) the grain-refining effect of Zr led to significantly smaller grains in the as-splatted material. The apparent retention of the Zr in solution up to $\sim$650K, and the maintenance of a finer grain size, offset some of the softening due to the breakdown of the network structure above $\sim$575K and the greatly improved strength above 600K is attributed to the precipitation of the Zr as small, metastable $ZrAl_3$ particles [35]. (It is to be emphasized at this point that, because of the highly variable microstructures throughout these alloys, a quantitative correlation with mechanical properties is extremely difficult.)

The Al–8% Fe–Mn Alloys also show improved tensile properties compared with the binary alloy (see Figs. 4, 12 and 13) but this is only true at temperatures below about 530K. This is attributed mainly to the higher volume fraction of second phase present and to the increased proportion of zone A grains which contained complete solid solution which probably precipitation hardened. The notable inferiority of the properties above this temperature is not easy to explain without further detailed work but is probably connected with the decomposition of the network zone A phase to globular incoherent (Fe, Mn)Al_6 particles, in contrast to the Al–8% Fe and Al–8% Fe–1% Zr alloys, which exhibited semi-coherent needles of $FeAl_3$. In addition, it was observed [35] that the (Fe, Mn)Al_6 particles coarsened more rapidly at 653K than did the $FeAl_3$ needles, which is related to both the more rapid diffusion of Mn compared to that of Fe in α-Al, and to the problem of relief of coherency strains around the $FeAl_3$ needles. The Al–5% Fe–3% Mn alloy was inferior in strength to all of the others; it exhibited a decreased rate of softening relative to Al–8% Fe in the range 280 to 450K, probably as a result of precipitation in as-splatted solid solution grains, but it is considered that the higher-temperature mechanical properties were inferior to those of the binary alloy because of the difference in decomposition behaviour which comes about by the addition of Mn.

In discussing this work it is worth examining the advantages of splat-cooling *vis-a-vis* conventional gas-atomization techniques for preparing high-strength alloys, by comparing the results obtained in the present work with those described by Towner [6, 7] for Al–8% Fe. Using gas-atomization, Towner prepared an Al–7.6% Fe-based alloy having a microstructure resembling zone B rather than zone A. Gas-atomization involves cooling rates $\sim 10^3$ K sec^{-1}. In the present work, cooling rates $\sim 10^6$ K sec^{-1} result in an Al–8% Fe alloy containing ~ 60% zone A, in which a very fine network structure with a cell spacing ~ 30 nm predominates. The splat-cooled structure results in an alloy with substantially higher room temperature strength. The strength of the splat-cooled alloy is also superior at all temperatures up to ~ 725K, where the properties are comparable (Fig. 9). At 725K splat-cooled Al–8% Fe has a predominantly zone B structure, following precipitation and subsequent coarsening of $FeAl_3$ needles in the zone A regions.

The properties of splat-cooled Al–8% Fe should also be compared with those for sintered aluminium powder products (SAP). Unlike SAP, the ductility of Al–8% Fe increases with increasing temperature. Thus acceptance of Al–8% Fe for high temperature applications need not be inhibited by the lack of ductility at high temperatures which resulted in the non-acceptance of SAP.

The acceptance of splat-cooled Al–8% Fe alloys for commercial applications depends on the forming characteristics, and the costs involved. Unfortunately the working temperatures for Al–8% Fe during forming are critical, and must be restricted to temperatures $\lesssim$ 575K to prevent excessive coarsening of the zone A network structure. In the extrusion process it has been demonstrated that a minimum specific pressure of 480 MN m^{-2} is necessary to achieve an extrusion ratio of 8:1. Hence to prepare large diameter extrusions, up to 5 cm diameter say, from ~ 15 cm diameter billets, a press with a minimum capacity of ~ 20 MN will be required. To prepare smaller diameter bar and wire from similar sized billets, non-conventional processes such as hydrostatic extrusion may be necessary.

5. Conclusions

1. Splat-cooled Al–8% Fe-based alloys, prepared by a bulk process and subsequently formed by compaction and extrusion, have been shown to have exceptional high temperature tensile properties and room temperature properties equivalent to those of the strongest aluminium alloys available. The tensile results suggest a maximum service temperature for Al–8% Fe of about 615K.

2. The stability of the as-splat-quenched microstructures of Al–8% Fe at temperatures up to ~ 615K is reflected in the long term tensile properties. The strength of the alloy after 1000 h exposure at temperatures up to ~ 725K is only slightly lower than after 1 h exposure at the same temperature.

3. The strength of splat-cooled Al–8% Fe is substantially superior to that of an Al–8% Fe alloy prepared by gas atomization, thus verifying the important potential of splat-cooling *vis-a-vis* gas atomization. The differences in strength can be directly attributed to the differences in cooling rate employed in these techniques.

4. Al–8% Fe has superior creep properties to established high temperature aluminium alloys such as RR58 and comparable fatigue and notch-impact properties.

5. Addition of 1% Zr to Al–8% Fe results in improved strength at all temperatures, and particularly between 575K and 725K. The strength of this alloy is unfortunately accompanied by a low room temperature ductility. Mn additions to Al–8% Fe improve the strength at temperatures between 375 and 525K thus, suggesting possibilities for developing new age-hardenable alloys.

6. Al–8% Fe-based alloys are not easily formable. Extrusion, for example, requires heavy equipment to produce fairly large sections: a press with a minimum capacity ~ 7 MN is required to produce ~ 2.5 cm diameter extruded bar. The working temperatures for these alloys must be restricted to $\lesssim$ 575K in order to prevent coarsening of the fine network structure within the zone A regions.

7. Applications for Al–8% Fe are likely to be in harsh high temperature environments where excellent high temperature tensile, fatigue and creep properties are essential, and where the materials must also withstand conditions likely to produce excessive erosion.

Acknowledgements

The authors are grateful to Drs D. A. Melford and M. H. Jacobs for stimulating discussions of this work, and to Mr J. J. Wintle for invaluable experimental assistance. This paper is published by permission of the Chairman of Tube Investments Ltd.

References

1. E. A. BLOCH, *Met. Rev.* **6** (1961) 193.
2. N. HANSEN, *Trans. Met. Soc. AIME* **230** (1964) 263.
3. H. KELLERER and G. PIATTI, *J. Mater. Sci.* **3** (1968) 222.
4. A. S. BUFFERD and N. J. GRANT, *Trans. Amer. Soc. Metals* **10** (1967) 305.
5. A. A. BRYUKHOVETS, N. N. BARBASKIN, M. G. STEPANOVA and I. N. FRIDLYANDER, *Poroshkovaya Metall* **1** (1970) 108.
6. R. J. TOWNER, *Metal Prog.* **73** (1958) 70.
7. *Idem, Metals Eng. Quart.* **1** (1961) 24.
8. H. M. SKELLY and C. F. DIXON, *Metal Prog.* **83** (1968) 103.
9. S. G. ROBERTS, in "Powder Metallurgy", edited by W. Leozynski (Interscience, New York, 1961) p. 7.
10. J. P. LYLE JUN., U.S. Patent 2 963 780, (1960).
11. T. F. BOWER, S. M. SINGH and M. C. FLEMINGS, *Met. Trans.* **1** (1970) 191.
12. T. R. ANANTHARAMAN and C. SURYANARAYANA, *J. Mater. Sci.* **6** (1971) 1111.
13. H. JONES, *Rep. Progr. Phys.* **36** (1973) 1425.
14. P. FURRER and H. WARLIMONT, *Z. Metallk.* **62** (1971) 12, 100.
15. P. DUWEZ and R. J. WILLENS, *Trans. Met. Soc. AIME* **227** (1963) 1581.
16. P. PIETROKOWSKY, *J. Sci. Instrum.* **34** (1963) 445.
17. P. ESSLINGER, *Z. Metallk.* **57** (1966) 109.
18. T. MASUMOTO and R. MADDIN, *Acta. Met.* **19** (1971) 725.
19. A. R. KAUFMANN and W. C. MULLER, in "Beryllium Technology", Vol. 1, (edited by L. M. Schetky and H. A. Johnson) (Gordon and Breach, New York, 1966), p. 629.
20. *Idem,* USAEC Report: NMI-1262, 1964.
21. *Idem,* USAEC Report: NMI-1263, 1965.
22. H. AHLBORN and D. MERZ, *Aluminium* **47** (1971) 671.
23. H. JONES and M. H. BURDEN, *J. Phys. E. Sci. Instrum.* **4** (1971) 671.
24. M. MOSS, *Acta Met.* **16** (1968) 321.
25. M. MOSS and D. M. SCHUSTER, *Trans ASM* **62** (1969) 201.
26. G. D. LAWRENCE and G. S. FOERSTER, *Int. J. Powder Met.* **6** (1970) 45.
27. N. J. GRANT, *Fizika* **2** (Suppl. 2) 16. Proceedings of the International Conference on Metastable Metallic Alloys, Brela, Yugoslavia 1970.
28. A. TONEJC and A. BONEFAČIČ, *J. Appl. Phys.* **40** (1969) 419.
29. H. JONES, *Mater. Sci. Eng.* **5** (1969/70) 1.
30. M. H. JACOBS, A. G. DOGGETT and M. J. STOWELL, *Fizika* **2** (Suppl. 2) 18. Proceedings of the International Conference on Metastable Metallic Alloys, Brela, Yugoslavia 1970.
31. A. FONTAINE, J. DIXMIER and A. GUINIER, *ibid,* p. 23.
32. G. THURSFIELD, H. JONES, M. H. BURDEN, R. C. DIBLING and M. J. STOWELL, *ibid,* p. 19.
33. G. THURSFIELD and H. JONES, *J. Phys. E. Sci. Instrum.* **4** (1971) 675.
34. W. M. DOYLE, *Metal Forming* **36** (1969) 216.
35. M. H. JACOBS, A. G. DOGGETT and M. J. STOWELL, *J. Mater. Sci.* **9** (1974) 1631.
36. D. TABOR, "The Hardness of Metals" (Clarendon Press Oxford, 1952) p. 15.
37. M. H. JACOBS A. G. DOGGETT and M. J. STOWELL, "Electron Microscopy and Analysis". Conference Series No. 10 (Institute of Physics, London and Bristol, 1971) p. 284.

Received 25 March and accepted 23 April 1974